Int. J. Nanosci. Nanotechnol., Vol. 13, No. 4, Dec. 2017, pp. 289-298

Large Vacuum Rabi Splitting in a Single Nitride-Based Quantum WellMicrocavity

Mehryar Alavi and Saeid Shojaei*

Department of Photonics, Research Institute for Applied Physics & Astronomy, University of Tabriz, Tabriz, Iran.

(*) Corresponding author: s_shojaei@tabrizu.ac.ir
(Received: 19 June 2016 and Accepted: 30 April 2017)

Abstract

Here, we report a theoretical detailed study of Vacuum Rabi Splitting (VRS) in the system of Nitride Single Quantum Well (SQW) within a semiconductor microcavity. Distributed Bragg Reflectors (DBRs) containing ZnTe/ZnSe multilayers including GaAs microcavity and $Al_xGa_{1-x}N/GaN/Al_xGa_{1-x}N$ ($GaN/In_xGa_{1-x}N/GaN$) SQW at the center of microcavity, has been considered. Upper and lower exciton-polariton branches obtained through angle-dependent reflectance calculations performed by the means of Transfer Matrix Method (TMM). Large value of 20.1(23.4) meV VRS is obtained by changing the Aluminum (Indium) molar fraction at the Room Temperature (RT) for TM mode. Our findings show that $GaN/In_xGa_{1-x}N/GaN$ SQW are better candidates rather than$Al_xGa_{1-x}N/GaN/Al_xGa_{1-x}N$ to achieve larger values of VRS. Our calculations pave the way towards modeling of polaritonic devices.

Keywords: *Vacuum Rabi Splitting, Exciton binding energy, Nitride semiconductors.*

1. INRODUCTION

Microcavity polaritons and especially polaritons based on Nitride nanostructures are good candidate for light matter coupling. Development of polariton's applications leads to the formation of field of polaritonics or polaritronics which is progressing with great speed [1]. Published articles in this field and generally nanotechnology and nanoscience are increasing dramatically and polariton microcavity promises many uses in various aspects of technology [2,3,4,5].The study of semiconductor microcavity started by pioneering works of C. Weisbuch et al in 1992 [6]. They observed vacuum Rabi splitting (VRS) for quantum well excitons by analogy to which had been observed for atomic systems [7]. This research leads to comprehensive researches in the field of strong coupling in intraction between light and matter in semiconductor microcavities during last two decades [8, 9, 10, 11, 12, 13]. Strong coupling and intraction between exciton and photon with same energy and momentum describes polariton quasi-particles. These states emerge from coherent energy exchange between quantum well excitons and cavity mode. One can assemble these materials vertically to fabricate optoelectronic devices which has enabled us to control light matter coupling. Polaritons are eigenstates as a result of strong light matter coupling. Exciton and photon are independent modes which has been tuned to each other by changing various parameters such as temperature [14], position of QW [6] and exposing electric [15] or magnetic field [16]. The cause of attention to these quasi-particles is their low in-plane effective mass around the center of first brillouin zone in quantum well nanostructures.

Nonlinear properties of polaritons provide the possibility of creation of the new generation of parametric optical amplifier and low threshold or even thresholdless lasing according to induced

scattering of polaritons [2] and polariton light emetting diodes by use of GaAs microcavity[17]. Since the exciton and photon are bosons these mixed states are bosons too, and are good candidate for Bose-Einstein Condensation (BEC) at high temperature [18] or even up to room temperature in GaN- based materials [19]. Generation of single photon source by use of coupled quantum dots [20], high temperature superconductivity [21] and control of switching which causes to reduce the bistability threshold to two or three orders of magnitude [22] are other advantages of application of these states. Also, motional narrowing in semiconductor microcavity is one of the research activity that has been started from 1996 [23]. It has been realized that InGaN QW with GaN barriers are good candidates to reach large VRS at RT. J. R. Chen et al observed 58 meV of VRS in a system containing AlGaN/ GaN as DBR and bulk ZnO-based hybrid microcavity as an active layer in which excitons are made[24]. G. Christmann et al reported 50mev large VRS for AlGaN/ GaN multiple quantum well at room temperature [25]. It has been suggested that, to reach larger VRS, double quantum well or even multi quantum wells are useful but enough attention should be paid to limitations of these systems such as saturation [26]. Microcavities contaning semiconductor quantum wells form a typical experimental systems that are very appropriate to study polariton physics. Amount of coupling strenghth depends on the geometry of studied system.

Nitride semiconductor based materials have significant applications in various fields of activity and research. Besides, GaN nanostructures have attracted a lot of interests because of their potential applications in photonic and optoelectronic devices [27, 28, 29]. Wide band gap in Nitride-based semiconductor makes them suitable materials for overcome the problem of short lifetime of cavity polaritons. This may makes more practical approach for room temperature operation. From the view point of strong coupling regime, they can be used as QWs [30] or DBRs [31].

In this work we consider ZnTe/ZnSe multilayer DBRs containing a GaAs microcavity between them and Nitride SQW at the center of microcavity. The estimation of VRS has been done theoretically to characterize the regime of strong coupling. We employ TMM to obtain the angle dependent reflectance spectrum. TMM has sum merits in this work. This method is suitable for multilayer systems and show the blue shift of cavity mode by varying the incident angle properly. Then the exciton binding energy will be calculated and finally the conditions of strong coupling regime and the variation in VRS values with relevant parameters will be studied in details. All of using parameters in this work to model the system are related to RT.

2. MODEL STRUCTURE

Our model structure is a SQW as $Al_xGa_{1-x}N/GaN/Al_xGa_{1-x}N$ and $GaN/In_xGa_{1-x}N/GaN$ embedded in a *GaAs* microcavity surrounded by *ZnTe/ZnSe* DBRs which is depicted in Figure 1.

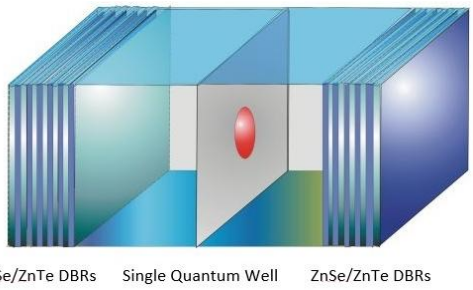

Figure 1*. A schematic view of Structure.*

By varying the width of the layers of DBRs, the cavity modes can be tuned. We choose the central wavelength as λ=570 nm and to hold the Bragg condition, thickness of layers as 46.4 and 54.2 nm that are of *ZnTe* and *ZnSe* respectively. We use a GaAs thin film as a defect layer at the center of the DBR acting as a 1D photonic crystal so that it's periodicity is perturbed. The thickness of the cavity is $\frac{\lambda}{2} = 285\text{nm}$

so this is a single mode cavity and for each half lambda increment in the cavity length one more cavity mode will be added to the number of cavity modes [9].We designed a Fabry-Perot cavity with DBR mirrors and put two excitonic structures as GaN SQW with $Al_xGa_{1-x}N$ barriers and $In_xGa_{1-x}N$ SQWwith GaN barriers at the center of the microcavity, x is the Aluminum or Indium molar fraction.

3. THEORETICAL PERSPECTIVE

3.1. Microcavity

Since DBRs are multilayer structures so it is appropriate to use TMM to calculate optical properties. One can use boundary conditions to formulate Maxwell equations and obtain transfer matrix for a single layer. Multiply the matrix of each layer successively gives final matrix for entire system. The matrix for normal incidence is written as:

$$M = \begin{pmatrix} coskl & \frac{-i}{n_1}sinkl \\ -in_1 sinkl & coskl \end{pmatrix} \quad (1)$$

Where, $n_1$and l are the refractive index and the length of the layer or thin film, respectively and k is the wave number. Following the final matrix as$M_{tot} = \begin{pmatrix} A & B \\ C & D \end{pmatrix}$, it can be shown easily that the reflection coefficient can be written as [26]:

$$r = \frac{An_0 + Bn_0n_T - C - Dn_T}{An_0 + Bn_0n_T + C + Dn_T} \quad (2)$$

Where n_0 and n_T are air and substrate refractive indices respectively. *A*, *B*, *C* and *D* are elements of resultant matrix *M*.

Figure1. depicts reflectance amplitude $R = rr^* = |r|^2$, of the *ZnTe/ZnSe* DBR at normal incidence with the 60nm stop band region from 540nm to 600nm which has approximately near 100% reflectance.

Hereafter, we concentrate on TM mode of oblique incidence. The transfer matrix for this mode has the below form:

$$M_{TM} = \begin{pmatrix} \cos(klcos\theta) & \frac{-i}{n_1/cos\theta}sin(klcos\theta) \\ -i(n_1/cos\theta)sin(klcos\theta) & cos(klcos\theta) \end{pmatrix} \quad (3)$$

For $\theta = 0$ it reduces to Eq. 1 .

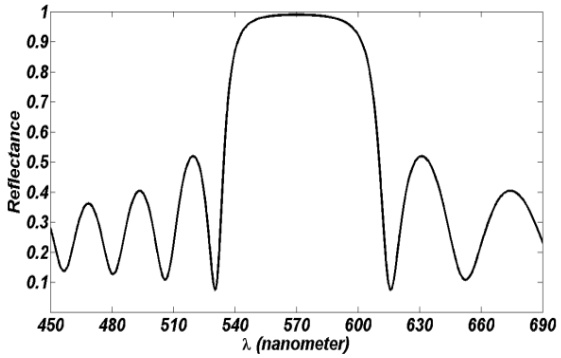

Figure 2*. DBR reflectance spectrum.*

Figure illustrates the reflectance diagram of a GaAs microcavity at normal incident of light without quantum well. The appeared deep shows the cavity mode with about 1nm line width.

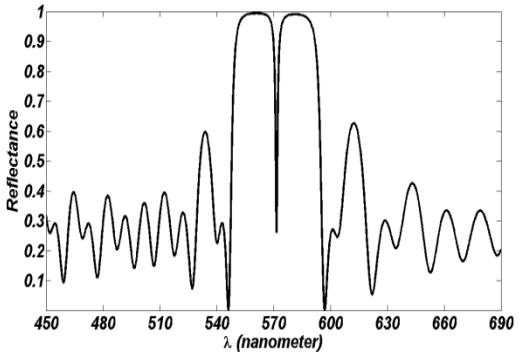

Figure 3. *Cavity reflectance spectrum.*

With increasing the incidence angle; the cavity mode is blue shifted governed by relation which has the below form [31]:

$$\omega_s = \frac{\pi c}{2}\frac{n_1cos\theta_2 + n_2cos\theta_1}{n_1n_2(d_1cos^2\theta_1 + d_2cos^2\theta_2)} \quad (4)$$

where θ_i , n_i , d_i are incidence angle, refractive index and thickness of ith layer, respectively.

Figure 4 illustrates the reflectance spectrum of ZnTe/ZnSe DBR for different values of incidence angles. It is clear that the position of cavity mode (position of dip) is shifted to shorter wavelength with increasing incidence angle. Tuning the cavity mode has key role in providing

resonance condition to observe exciton-polariton.

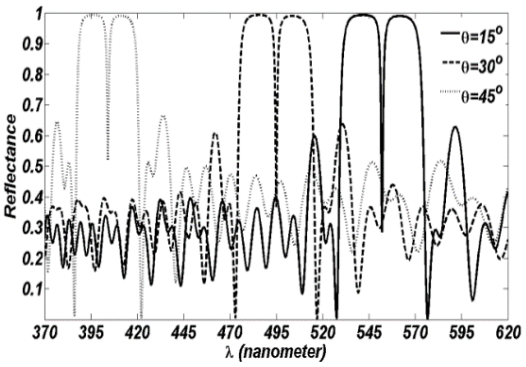

Figure 4*. Variation of cavity mode by varying incident angles.*

3.2. Exciton

In the transfer matrix formalism we need to know the amount of refractive index of quantum well layer where exciton forms. One can use Lorentz model and calculate the refractive index as below [33]:

$$\varepsilon(E) = n^2(E) = \varepsilon_\infty + \frac{fq^2h^2}{m\varepsilon_0 L_z}\frac{1}{E_0^2 - E^2 - i\gamma E} \qquad (5)$$

where ε_∞ is dielectric constant at high frequencies, f is exciton oscillator strength per unit area, q is the electron charge, h is plank's constant, m is the vacuum electron mass, ε_0 is the vacuum dielectric constant, L_z is the width of well, E_0 is exciton transition energy, E is the energy of cavitymode and γ is exciton homogeneous linewidth.

To calculate exciton transition energy, exciton Hamiltonian can be written as:

$$H_{exc} = H_e + H_h + H_{int} \qquad (6)$$

In Eq. 6 H_e and H_h are the electron and hole parts of Hamiltonian, respectively. H_{int} is the interaction part of Hamiltonian originates from coulomb interaction between electron and hole because of opposite charge of the electron and hole. In the effective mass approximation the Hamiltonian describing the electron and hole in a QW which is grown in z direction reads:

$$H_i = -\frac{\hbar^2}{2}\nabla_i\left(\frac{1}{m_i^*(x_i.y_i.z_i)}\nabla_i\right) + V_i(z_i) \qquad (7)$$

Index $i = e$ and $i = h$refers to electron and hole, respectively. The potential $V_i(z_i)$ is confinement potential and accounts for the band offset which is originates from energy gap difference of QW materials. Third term of right hand side of Eq.6 is related to electron-hole coulomb interaction and is written as:

$$H_{int} = -\frac{e^2}{4\pi\varepsilon\sqrt{(x_e - x_h)^2 + (y_e - y_h)^2 + (z_e - z_h)^2}} \qquad (8)$$

In cylindrical coordinates the Hamiltonian is:

$$H_{exc} = H_{ez} + H_{hz} - \frac{\hbar^2}{2\mu}\left[\frac{1}{\rho}\frac{\partial}{\partial\rho}\left(\rho\frac{\partial}{\partial\rho}\right) + \frac{1}{\rho^2}\frac{\partial^2}{\partial\varphi^2}\right] - \frac{e^2}{4\pi\varepsilon\sqrt{\rho^2 + z^2}} \qquad (9)$$

where $\rho = \sqrt{x^2 + y^2}$is the radius coordinate in cylindrical coordinates and x and y are relative coordinates of electron and hole i.e. $x = x_e - x_h, y = y_e - y_h$. H_{ez} and H_{hz} are electron and hole Hamiltonian in the quantum well and has the below form:

$$H_{ez} = -\frac{\hbar^2}{2}\frac{\partial}{\partial z_e}\left(\frac{1}{m_e^*(z_e)}\frac{\partial}{\partial z_e}\right) + V_e(z_e) \quad . \qquad (10)$$

Also the effect of the built-in electric field should be considered. It is induced by spontaneous and piezoelectric polarization which take place in nitride materials. They can be considered by:

$$F_w^z = \frac{P_b^{sp} + P_b^{pz} - P_w^{sp} - P_w^{pz}}{\varepsilon^w + \varepsilon^b\left(\frac{L_w}{L_b}\right)} \qquad (11)$$

$$F_b^z = -\frac{L_w}{L_b}F_w^z \qquad (12)$$

where index w and b are related to well and barrier region, sp and pz are related to spontaneous and piezoelectric polarization, respectively; Finally, $\boldsymbol{L_w(L_b)}$ is the well (barrier) width. Table 2 shows the relation between parameters $\mathbf{C_{13}}$,$\mathbf{C_{33}}$, elements of elastic tensors, $\mathbf{e_{33}}$,$\mathbf{e_{31}}$,piezoelectric constants, and $\boldsymbol{\varepsilon_{31}}$, the dielectric constant, with spontaneous and piezoelectric polarizations, $\boldsymbol{P^{pz}}$ and $\boldsymbol{P^{sp}}$[33]. Hereafter, we take $\boldsymbol{L_b = 2L_w}$.

Exciton Oscillator Strength (EOS) reads:

$$f = \frac{2M^2}{m_0 E_{exc}}\left|\int_{-\infty}^{+\infty} dz f_e(z) f_h(z)\right|^2 |\Phi(0)|^2 \qquad (13)$$

where M is the optical transition matrix element between the valence and conduction bands. $f_e$and f_h are the envelope functions of electrons and holes in the z direction (perpendicular to the surface).

$\Phi(r)$ describes the relative motion of the electron and hole in the x-y plane, and $\Phi(0)$ denotes the probability of finding electrons and holes at the same position and $E_{exc}$is exciton binding energy and m_0 is free electron mass [34]. The value of EOS is proportional to the coupling strength so that with increasing the EOS, VRS increases and as a result, coupling strength increases that is needed to reach strong coupling regime [26].

The physical parameters are introduced in Table. 1.

Table 1. *Physical parameters of AlN, GaN, InN [30].*

Parameters	AlN	GaN	InN
$a_0(A^\circ)$	3.112	3.189	3.54
$e_{33}(C/m^2)$	1.46	0.73	0.97
$e_{31}(C/m^2)$	-0.60	-0.49	-0.57
$C_{13}(GPa)$	108	103	121
$C_{33}(GPa)$	373	405	182
ε_{31}	10.1	10.4	15.3
$P^{sp}(C/m^2)$	-0.081	-0.029	-0.032
$E_g(ev)$	6.2	3.4	2.0

To calculate the energy gap of Nitrides alloys, we use Vegard's law as below [36]:

$$E_g^{A_xB_{1-x}N} = E_g^{BN}(1-x) + E_g^{AN}x - bx(1-x) \quad (14)$$

where b is bowing factor which is b=1ev for $Al_xGa_{1-x}N$[30] and b=2.5ev for$In_xGa_{1-x}N$[37].

Table 2. shows the relations used to calculate nitride semiconductor parameters.

Figure 5 shows band profile of the$In_xGa_{1-x}N$QW with *GaN* barriers where x=0.15 has been considered. First three levels wavefunction depicted.

The ground state is the lowest level with one peak and the first and second excited state are depicted respectively from down to up. In all of these states the probability of existing of electron in right hand side is more than the left hand side and this is because of piezoelectric and spontaneous electric fields.

Figure 5 shows band profile of the$In_xGa_{1-x}N$QW with *GaN* barriers where x=0.15 has been considered. First three levels wavefunction depicted.

Table 2. *Physical parameters of AlN, GaN, InN as function of Aluminum and Indium molar fraction [30, 32]*

Parameters	$Al_xGa_{1-x}N$	$In_xGa_{1-x}N$
$a_0(A^\circ)$	$-0.077x + 3.189$	$0.351x + 3.189$
$e_{33}(C/m^2)$	$[e_{33}(AlN) - e_{33}(GaN)]x + e_{33}(GaN)$	$[e_{33}(InN) - e_{33}(GaN)]x + e_{33}(GaN)$
$e_{31}(C/m^2)$	$[e_{31}(AlN) - e_{31}(GaN)]x + e_{31}(GaN)$	$[e_{31}(InN) - e_{31}(GaN)]x + e_{31}(GaN)$
$C_{13}(GPa)$	$5x + 103$	$18x + 103$
$C_{33}(GPa)$	$-32x + 405$	$-223x + 405$
ε_{31}	$-0.3x + 10.4$	$3.9x + 10.4$
$P^{sp}(C/m^2)$	$-0.052x - 0.029$	$-0.003x - 0.029$
$P^{pz}(C/m^2)$	$2\left[\frac{a_s(x)-a(x)}{a(x)}\right][e_{31}(AlN) - e_{33}(GaN)\frac{C_{13}(x)}{C_{33}(x)}]$	$2\left[\frac{a_s(x)-a(x)}{a(x)}\right][e_{31}(InN) - e_{33}(GaN)\frac{C_{13}(x)}{C_{33}(x)}]$

The ground state is the lowest level with one peak and the first and second excited state are depicted respectively from down to up. In all of these states the probability of existing of electron in right hand side is

more than the left hand side and this is because of piezoelectric and spontaneous electric fields.

4. RESULTS AND DISCUSSIONS

Figure 6 shows the variation of exciton binding energy versus quantum well width. Hereafter we take the barrier width 30A° and Aluminum (Indium) molar fraction as $x = 0.15$. It can be seen that the value of binding energy is quite low for small well width, it then increases and attains a maximum after which it decreases.

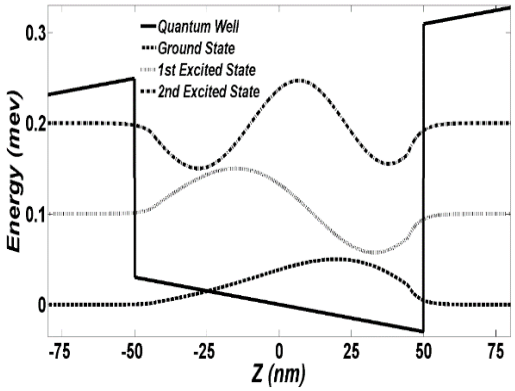

Figure 5. *Band profile of* $\boldsymbol{GaN/In_{015}Ga_{0.85}N/GaN}$ *quantum well and the wavefunction of ground states, 1st and 2nd excited states.*

For large well width the binding energy tends to bulk value. With a reduction of well width, the orbit gets squeezed and reduced separation between the pairs (electron, hole) gives rise to large binding energy. The trend of increasing binding energy with decreasing width continues up to a width of about 4nm. From Figure 6 it is clear that exciton binding energy for InGaN QW is larger than that of GaN QW and this is because of quantum confinement effect.

For GaN SQW with 10nm well width Figure7 shows the cavity dip around 3332 meV which has varied by increasing the angle of incidence. The relevant dip of QW structure resonance starts to be appeared from right at 3385 meV.

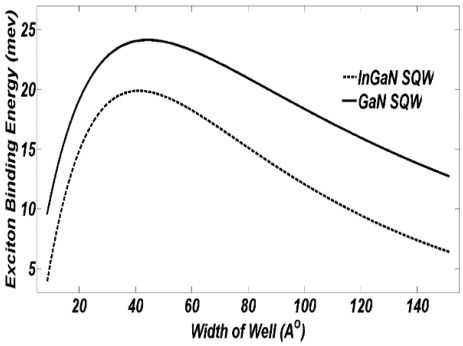

Figure 6. *Exciton binding energy in* $Al_{0.15}Ga_{0.85}N/GaN/Al_{0.15}Ga_{0.85}N$ *and* $GaN\ /\ In_{0.15}Ga_{0.85}N/\ GaN$ *SQWs.*

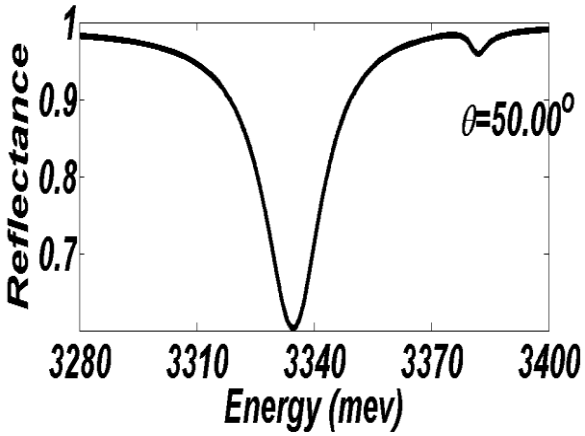

Figure 7*. Appearance of quantum well resonance at* $\mathbf{50.00°}$.

With increasing the incidence angle VRS can be observed with the amount of 18.6 meV at the incidence light angle of around $50°$ as depicted in Figure8.

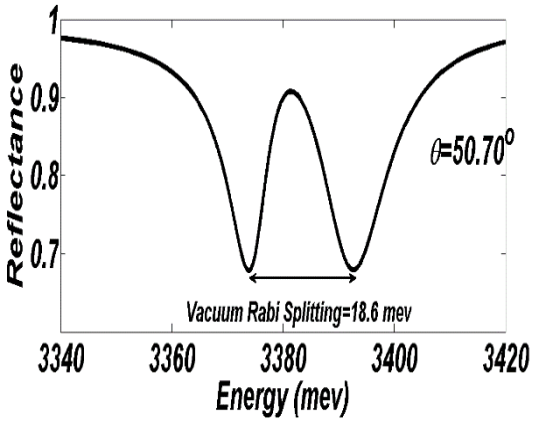

Figure 8. *Vacuum Rabi Splitting in GaN QW in resonant condition.*

Figure 9 illustrates that increasing the incidence angle of light to the about $51.40°$ the relevant dip of quantum well structure moves to lower energy that is attributed to lower branch of polaritons.
Figure 10 shows the calculated angle resolved reflectance spectrum of system of GaN SQW and above mentioned microcavity. The lowest curve is related to the $\mathbf{50.00°}$ light incidence angle. Other curves obtained by adding $\mathbf{0.10°}$to the value of angle.

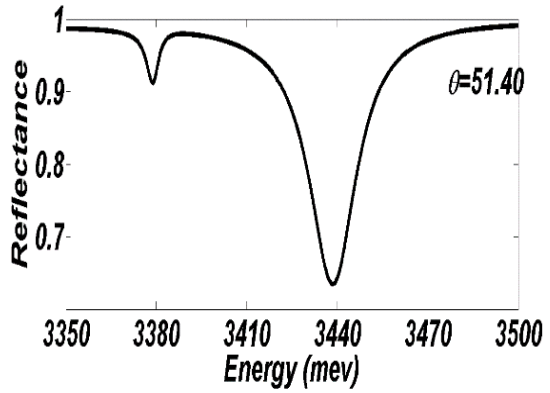

Figure 9. *Reflectance spectrum of GaN QW and microcavity at the light incident angle of* $\mathbf{51.40°}$.

We observed that with increasing the angle of incident light, coupling strength becomes stronger. The dashed curve is related to $\mathbf{50.70°}$ which shows the strongest coupling regime where normal mode coupling occurs. The angle related to strong coupling is called resonant angle (50.70) and with increasing the angle of incidence, coupling strength reduces again and exciton bleaching occurs.

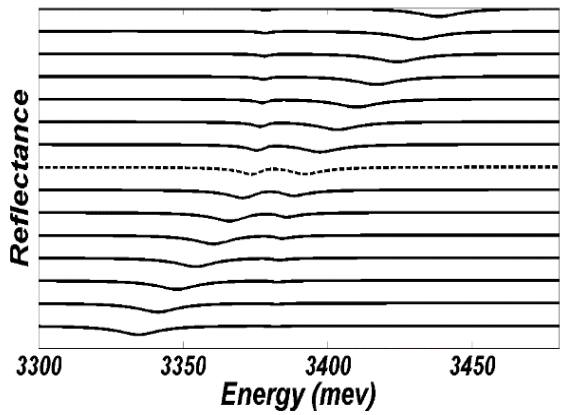

Figure 10. *Calculated angle resolved reflectance Spectrum.*

Figure11 depicts the dip positions of reflectance spectrum in Figure10 versus angle of incident light. Higher (lower) energy form Upper (Lower) polariton branch, UPB (LPB). Also it has been shown that at lower angles of incident light, UPB has exciton-like behavior and LPB has photon-like behavior in opposite to higher incidence angles where LPB has exciton-like behavior and UPB has photon-like behavior. Around the resonant angle of $50.70°$ the behavior of the system is not bare exciton-like or bare photon-like and this behavior introduce the new quasi particles, exciton-polariton [5].

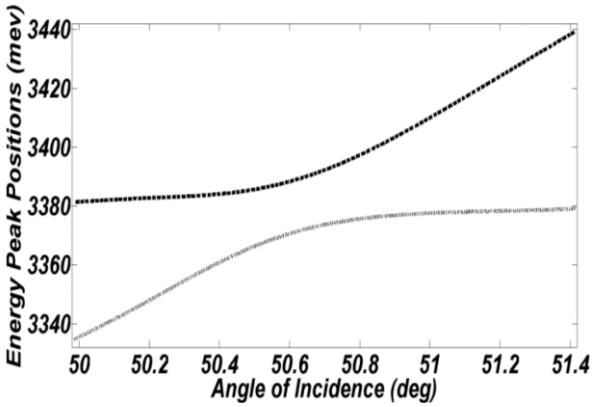

Figure 11. *UPB & LPB in the system of GaN SQW-microcavity.*

Figure12 shows the behavior of VRS versus molar fraction of Aluminum for different well widths. It can be seen that VRS increases with increasing Aluminum molar fraction that is because of enhancement of exciton binding energy with increasing x. Also, it is found that larger values of VRS can be obtained in the case of thinner QWs due to the larger exciton binding energy as discussed in Figure 6.

In Figure 13 it has been shown that the variation of VRS as a function of Indium molar fraction in $GaN/In_xGa_{1-x}N/GaN$ SQW. It can be seen that there is the same behavior as depicted in Figure12 observed but the value of VRS is larger.

To compare our findings with other works, we considered the work of T. Tawara et al [30], where they obtained 17meV VRS in InGaN quantum well

microcavities at room temperature. Our proposed model structure gives larger values of VRS needed for high performance polaritonic devices.

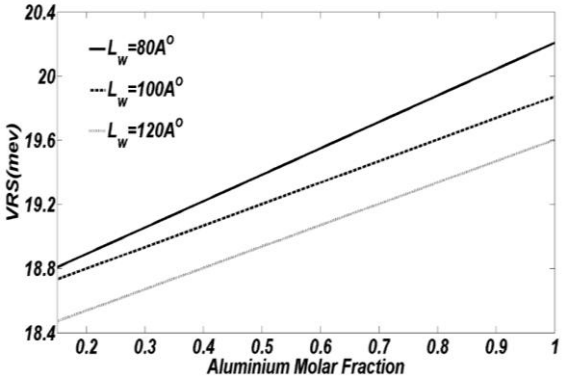

Figure 12. *VRS as a function of Aluminum molar fraction for* $\boldsymbol{Al_xGa_{1-x}N/GaN/AlxGa1-xN}$*SQW*

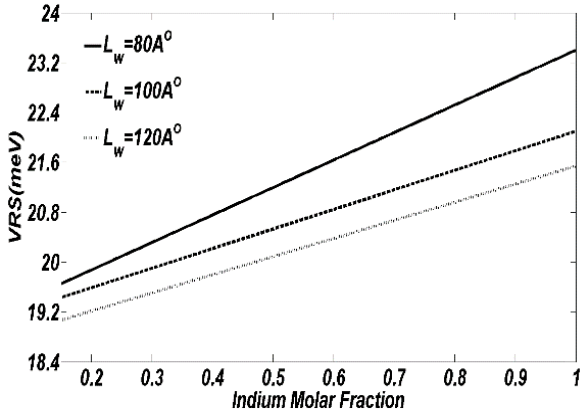

Figure 13. *VRS as a function of Indium molar fraction for* $\boldsymbol{GaN/In_xGa_{1-x}N/GaN}$*SQW.*

Figure 14. shows the variation of VRS with well width where molar fraction is taken same in both systems as x=0.9. It is clear that VRS increases with increasing well width and reaches a maximum and then decreases with increasing width of well. The maximum VRS occurs at around 3nm of well width. This behavior can be described by the behavior of exciton binding energy with increasing the well width as depicted in Figure 6. In fact, quantum confinement effect results in enhancement of exciton binding energy and providing the strong confinement regime.

5. CONCLUSION

In summary, we studied the angle-dependent reflectance spectrum in the formalism of Transfer Matrix Method (TMM) theoretically.

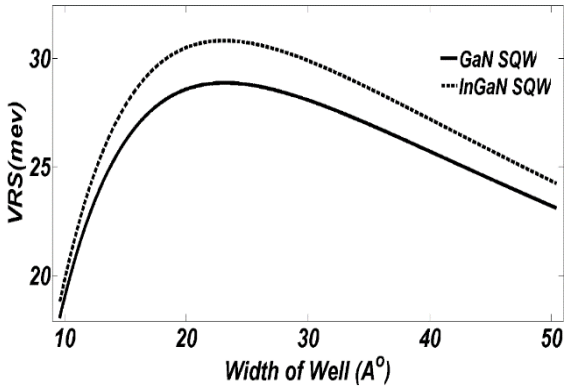

Figure 14*. Effect of well width changing on VRS for x=0.9 molar fraction.*

This study has been done in order to study the weak and strong coupling regime and Vacuum Rabi splitting (VRS) in a polariton microcavity which is containing a single mode GaAs microcavity with single quantum well. Two kinds of QWs as $Al_xGa_{1-x}N/GaN/Al_xGa_{1-x}N$ and $GaN/In_xGa_{1-x}N/GaN$ has been considered. We found that by changing the geometry of the system such as Indium (Aluminum) molar fraction or width of well we can achieve the considerable value of VRS by using $GaN/In_xGa_{1-x}N/GaN$ SQW. All parameters used in this work to model the system are in room temperatures. Critical value of well width obtained at which the VRS is maximum. Our proposed structure is promising for polariton based devices such as polariton LED, Polariton lasers and polariton switches operating at room temperature. Also, our calculations pave the ways toward modeling of polaritonic devices.

REFERENCES

1. Kavokin, A. (2009). "Optical switching: "Polariton diode microcavities", *Nature Photonics*, 3: 135-136.

2. Savvidis, P. G. (2014). “Optoelectronics: A practical polariton laser”, *Nature Photonics*, 8: 588-589.
3. Byrnes, T, Kim, N. Y, Yamamoto, Y. (2014). “Exciton–polariton condensates”, *Nature Physics*, 10: 803-813.
4. Moezzi, A, Soltanali, S, Torabian, A. H, Hasani, A. (2017). “Removal of Lead from Aquatic Solution Using Synthesized Iron Nanoparticles”, *Int. J. Nanosci. Nanotechnol*, 13 (1): 83-90.
5. Salehian, M, Mohammadian, A, Vaezzadeh, M, Saeidi, M, Hasani, A. H. (2017). “Influence of Size on the Melting Temperatureof Metallic Nanoparticl”, *Int. J. Nanosci. Nanotechnol*, 13(1): 91-95.
6. Weisbuch, C, Nishioka, M, Ishikawa, A, Y, Arakawa, Y. (1992). “Observation of the coupled exciton-photon mode splitting in a semiconductor quantum microcavity”, *Phys. Rev. Lett*, 69: 3314.
7. Zhu, Y, Gauthier, D. J, Morin, S. E, Wu, Q, Carmichael, H. J, Mossberg, T. W. (1990). “Vacuum Rabi splitting as a feature of linear-dispersion theory: Analysis and experimental observations”, *Phys. Rev. Lett*, 64: 2499-2502.
8. Houdre, R, Weisbuch, C, Stanley, R. P, Oesterle, U, Pellandini, Ilegems, M, (1994). “Measurement of cavity-polariton dispersion curve from angle resolved photoluminescence experiments”, *Phys. Rev. Lett*, 73: 2043-2046.
9. Abram, I, Oudar, J. L, (1995). “Spontaneous emission in planar semiconductor microcavities displaying vacuum Rabi splitting”, *Phys. Rev. A*, 51: 4116-4122.
10. Tim Byrnes, Na Young Kim,Yoshihisa, Y. (2014). “Exciton-polariton condensate”, *Nature Physics*, 10: 803-813.
11. Gerace, D, Andreani, L. C, (2007). “Quantum theory of exciton-photon coupling in photonic crystal slabs with embedded quantum wells”, *Phys. Rev. B*, 75: 23532501-23532512.
12. Dupont, E, Gupta, J. A, Liu, H. C, (2007). “Giant vacuum-field Rabi splitting of intersubband transitions in multiple quantum wells”, *Phys. Rev. B*, 75: 20532501-20532505.
13. Dufferwiel, S, Schwarz, S, Withers, F, Trichet, A. A. P, Li, F, Sich, M, Del Pozo-Zamudio, O, Clark, C, Nalitov, A, Solnyshkov, D. D, Malpuech, G, Novoselov, K. S, Smith, J. M, Skolnick, M. S, Krizhanovskii, D. N, Tartakovskii, A. I, (2015). “Exciton–polaritons in van der Waals heterostructures embedded in tunable microcavities”, *Nature Communications*, 6: 1-7.
14. Pau, S, Björk, G, Jacobson, J, Cao, H, Yamamoto, Y. (1995). “Microcavity exciton-polariton splitting in the linear regime”, *Phys. Rev. B*, 51: 14437-14447.
15. Fisher, T. A, Afshar, A. M, Whittaker, D. M, Skolnick, M. S, Roberts, J. S, Hill, G, Pate, M. A, (1995). “Electric-field and temperature tuning of exciton-photon coupling in quantum microcavity structures”, *Phys. Rev. B*, 51: 2600-2603.
16. Piętka, B, Zygmunt, D, Król, M, Molas, M. R, Nicolet, A. A. L, Morier-Genoud, F, Szczytko, J, Lusakowski, J, Zieba, P, Tralle, I, Stępnicki, P, Matuszewski, M, Potemski, M, Deveaud, B, (2015). “Magnetic field tuning of exciton-polaritons in a semiconductor microcavity”, *Phys. Rev. B*, 91: 07530901-07530910.
17. Bajoni, D, Semenova, E, Lemaitre, A, Bouchoule, S, Wertz, E, Senellart, P, Bloch, J, (2008). “Polariton light-emitting diode in a GaAs-based microcavity”, *Phys. Rev. B*, 77: 11330301-11330304.
18. Deng, H, Haug, H, Yamamoto, Y, (2010). “Exciton-polariton Bose-Einstein condensation”, *Rev. Mod. Phys* 82: 1489-1537.
19. Malpuech, G, Carlo, A. D, Kavokin, A, Baumberg, J. J, Zamfirescu, M, Lugli, P, (2002). “Room-temperature polariton lasers based on GaN microcavities”, *Appl. Phys. Lett*, 81: 412-414.
20. Liew, T. C. H, Savona, V, (2010). “Single Photons from Coupled Quantum Modes”, *Phys. Rev. Lett*, 104: 18360101-18360104.
21. Laussy, F. P, Kavokin, A. V., Shelykh, I. A, (2010). “Exciton-polariton mediated superconductivity”, *Phys. Rev. Lett*, 104: 10640201-10640204.
22. Baas, A, Karr, J. Ph, Eleuch, H, Giacobino, E, (2004). “Optical bistability in semiconductor microcavities”, *Phys. Rev. A*, 69: 02380901-02380908.
23. Whittaker, D. M, Kinsler, P, Fisher, T. A, Skolnick, M. S, Armitage, A, Afshar. A. M, Sturge, M. D, Roberts, J. S, (1996). “Motional Narrowing in Semiconductor Microcavities”, *Phys. Rev. Lett*, 77: 4792-4796.
24. Chen, J. R, Lu, T. C, Wu, Y. C, Lin, S. C, Liu, W. R, Hsieh, W. F, Kuo, C. C, Lee, C. C, (2009*). App. Phys. Lett*, 94: 061103-061109.
25. Christmann, G, Butte, R, Feltin, E, Mouti, A, Stadelmann, P. A, Castiglia, A, Carlin, J. F, Grandjean, N, (1995). “Large vacuum Rabi splitting in a multiple quantum well GaN-based microcavity in the strong-coupling regime”, *Phys. Rev. B*, 77: 08531001-08531009.
26. Kavokin, A, Malpuech, G. (2003). “*Thin Films and Nanostuctures: Cavity Polaritons*”, Elsevior, Netherlands.
27. Morkoc, H. (2008). “*Handbook of Nitride Semiconductors and Devices*”, Wiely, USA.
28. Patil, D. S, Talele, K, Samuel, E. P, Sonawane, U. S, (2016). “Self-consistent analysis of electron transport in GaN/AlGaN super lattice nanostructure for light emission”, *Optik*, 127: 7374-7381.
29. Talele, K, Samuel, E. P, Patil, D. S, (2011). “Analysis of carrier transport properties in GaN/Al0.3Ga0.7N multiple quantum well nanostructures”, *Optik*, 122: 626-630.

30. Tawara, T, Gotoh, H, Akasaka, T, Kobayashi, N, Saitoh, T, (2004). "Cavity Polaritons in InGaN Microcavities at Room Temperature", *Phys. Rev. Lett*, 92: 256402-256406.
31. Panzarini, G, Andreani, L. C, Armitage, A, Baxter, D, Skolnick, M. S, Roberts, J. S, Astratov, V. N, Kaliteevski, M. A ,Kavokin, A. V, Vladimirova, M. R, (1999). "Cavity–Polariton Dispersion and Polarization Splitting in Single and CoupledSemiconductor Microcavities", *Phys. Sol. Stat.*, 41: 1223-1237.
32. Fowls, G. R. (1975). "*Introduction to Modern Optics*", Dover Publications, London.
33. Houdre, R, Stanley, R. P, Oesterle, U, Ilegems, M, (1994). "Room-temperature cavity polaritons in a semiconductor microcavity", *Phys. Rev. B*, 49:16761-16764.
34. Zhang, B, Kano, S. S, Shiraki, Y, Ito, R, (1994). "Reflectance study of the oscillator strength of excitons in semiconfiuctor quantum wells", *Phys. Rev. B*, 50: 7499-7501.
35. Bernardini, F, Fiorentini, V, Vanderbilt, D, (1997). "Spontaneous polarization and piezoelectric constants of III-V nitrides", *Phys. Rev. B*, 56: R10 024-R10 027.
36. Pela, R. R, Caetano, C, Marques, M, Ferreira, L. G, Furthmüller, J, Teles, L. K, (2011). "Accurate band gaps of AlGaN, InGaN, and AlInN alloys calculations based on LDA-1/2 approach", *Appl. Phys. Lett*, 98: 151907.
37. Shojaei, S, Troiani, F, Asgari, A, Kalafi, M, Goldoni, G. (2008). "Coulomb-InducedNonlinearities in GaN Microdisks", *Eur. Phys. J. B*, 65: 505.